

# Real-life Implementation and Comparison of Authenticated Path Following for Automated Vehicles based on Galileo OSNMA Localization

Selim Solmaz\*, *Senior Member, IEEE*  
Control Systems Group (Dept.-E)  
Virtual Vehicle Research GmbH  
Graz, 8010 Austria  
selim.solmaz@v2c2.at

Georg Nestlinger\*  
Control Systems Group (Dept.-E)  
Virtual Vehicle Research GmbH  
Graz, 8010 Austria  
georg.nestlinger@v2c2.at

Karl Diengsleder-Lambauer  
Embedded Systems Group (Dept.-E)  
Virtual Vehicle Research GmbH  
Graz, 8010 Austria  
karl.lambauer@v2c2.at

Roman Lesjak  
Joanneum Research Forschungs GmbH  
Graz, 8010 Austria  
roman.lesjak@joanneum.at

Susanne Schweitzer  
Joanneum Research Forschungs GmbH  
Graz, 8010 Austria  
susanne.schweitzer@joanneum.at

José M. Vallet García  
Finnish Geospatial Research Institute  
Espoo, Finland  
jose.vallet@nls.fi

**Abstract**—We present a comparative analysis of EGNSS-based path tracking with and without open service navigation message authentication (OSNMA), which was recently made available in mass market EGNSS (Galileo) receivers. The EGNSS receivers provide dual-band GPS L1/L2 and Galileo E1/E5a RTK positioning for cm-level GNSS localization. The path following task utilizes mainly the accurate RTK-assisted EGNSS position and heading information to track a reference path. The lateral error from the reference path is used as the correction signal for the tracking controller. We compare the performance of the tracking controller in an open-sky and urban setting within the Graz University of Technology Inffeldgasse campus using an automated driving demonstrator vehicle. The positioning utilized two different OSNMA schemes, namely “strict” OSNMA solution that utilize only authenticated Galileo satellites or not using authentication, implying utilisation of all the available GNSS satellites.

**Index Terms**—EGNSS, Galileo, OSNMA, authenticated localization, path following.

## I. INTRODUCTION

In recent years, there has been a lot of interest in and progress with automated vehicles (AVs). While there are numerous technological and regulatory obstacles to overcome before completely autonomous traffic is realized, one of the most significant expectations for AVs is to maintain safety and confidence.

To ensure a more complete understanding of the environment and use it as the foundation for reliable judgments, the majority of AVs use a multitude of sensors and ECUs. Most of the time, the data from the onboard sensors and HD maps amounts to giving the vehicle a baseline trajectory and speed to follow. Sensors are used by perception systems to collect data in real time and identify objects, while trajectory planning algorithms determine the best course after taking into

account a number of criteria. Vehicle control systems translate the intended course into vehicle movements, guaranteeing adherence to it and keeping the vehicle at a safe distance from obstacles.

On the other hand, localization enables vehicles to identify their exact location inside the outside world, which is an indispensable component of highly-automated driving systems. To ensure higher levels of autonomy in the sense of the widely accepted SAE J3016 norm [1], accurate localization is needed, which typically uses GNSS receivers and IMUs.

The ESRIUM project [2] in general investigates various aspects of highly accurate, reliable, and assured EGNSS localization information for road vehicles with a particular focus on automated vehicles. Opportunities of utilizing C-ITS infrastructure and EGNSS-based localization in planning trajectories of automated vehicles are addressed [3], [4]. The overall aim is to set up a service to foster greener and smarter road usage and maintenance, as well as to increase road safety, e.g., by creating a map of road damage and associated safety risks at centimetre-level resolution. Precise localization is a prerequisite to achieving this task. Several aspects of RTK+OSNMA positioning performance are investigated within the project.

In the current paper, we present a comparative analysis of an EGNSS-based path tracking system with and without open service navigation message authentication (OSNMA), which was recently made available in mass market EGNSS (Galileo) receivers. In order to enhance the security of the EGNSS-based localization systems supporting the OSNMA service, this particular subject is being researched as part of the ESRIUM project. By using the authenticated positioning supported by OSNMA, this can in turn increase the robustness and reliability of autonomous driving systems.

The EGNSS receivers provide dual-band GPS L1/L2 and

\*Selim Solmaz and Georg Nestlinger are co-first authors.



Figure 1. Automated Driving Demonstrator (ADD) vehicle antenna configuration during the path following experiments.

Galileo E1/E5a RTK positioning for cm-level GNSS localization. The trajectory-following task utilizes mainly the accurate RTK-assisted EGNSS position and heading information to track a reference path. The lateral error from the reference path is used as the correction signal for the tracking controller. We compare the performance of the tracking controller in an open-sky and urban setting within the Graz University of Technology Inffeldgasse campus using an automated driving demonstrator vehicle. The positioning utilized two different OSNMA schemes, namely “strict” OSNMA solution that utilizes only authenticated Galileo satellites or not using authentication, implying utilisation of all the available GNSS satellites.

The rest of this paper is structured as follows. Section II describes the test vehicle and measurement setup in detail. This is followed by the description of the path following use case as well as the longitudinal/lateral control methods and the reference path selection approach in Section III. In Section IV the test results are presented followed by a short discussion for each test case. The final conclusions and outlook are then given in Section V.

## II. TEST VEHICLE SETUP

The test vehicle is a Ford Mondeo Hybrid. The vehicle state is accessible via CAN bus and provides measurements such as accelerations, speed, yaw rate, etc. Additionally, drive-by-wire can be accomplished by controlling a desired steering wheel angle along with brake/throttle commands. For this specific study, several GNSS receivers and antennas were installed in addition to the permanently installed Novatel setup, see Figure 1. For the closed-loop path following as described in Section III, the Septentrio mosaic-H5 dual-antenna EGNSS receiver was used, while the logged data of the Septentrio mosaic-X5 single antenna receivers was used for the purpose of comparison. In detail, we used a test setup with the following components:

- Septentrio mosaic-H with dual antenna-setup
- Tallysman TW7972 antennas.
- Septentrio mosaic-X5 (development kit)
- Septentrio mosaic-X5 Go
- Novatel ProPak 6 RTK D-GPS
- iMAR iNAT-FSLG-01 inertial measurement system
- NavXperience 3G+C multi-band GNSS antenna
- 1-by-4 antenna splitter (ALDCBS1X4)

The Automated Driving Demonstrator (ADD) vehicle is equipped with several additional sensors, computational hardware, and custom software components. The ADD vehicle is fitted with the DataSpeed drive-by-Wire Kit<sup>1</sup>, which enables access to CAN data as well as the drive-by-wire actuators. The ADD Vehicle is also equipped with additional sensors, which can be modified depending on the measurement or the use-case requirements. These additional sensors include superfluous combinations of cameras, radar, lidar, and GNSS receivers. The vehicle also includes a number of computational platforms that include a vehicle-grade high-performance Intel PC, a dSPACE MicroAutoBox II real-time ECU, and an Nvidia Drive PX/2 ADAS PC. These several redundant hardware, sensors, and platforms are the reason for the cluttered booth space, seen in Figure 2.



Figure 2. Automated Driving Demonstrator (ADD) vehicle based on the Ford Mondeo 2016 platform and DataSpeed drive-by-wire interface. The ADD vehicle is equipped with rudimentary EGNSS receiver/antenna configurations to analyse the effect of OSNMA on tracking performance.

In Figure 1, one can see several antennas on the roof as well as the redundant hardware in the boot space (Figure 2), which are not all relevant to this paper. In the center of the roof, one can see the white and light blue GNSS antenna, which is a NavXperience 3G+C geodetic multi-frequency GNSS antenna. The white antenna on the rear window is the

<sup>1</sup><https://www.dataspeedinc.com/>

4G antenna (NETVIP 4G TS9 35dBi LTE antenna). Figure 3 shows a schematic of the whole localization setup where the GNSS antenna is connected to an active 1-by-4 antenna splitter (ALDCBS1X4), which shares the signal between two Septentrio mosaic X5 mass-market multi-frequency GNSS receivers and a tactical-grade iMAR iNAT-FSLG-01 GNSS/IMU system for validation purposes. The mosaic X5 receiver was configured to track only GPS L1/L2 and Galileo E1/E5a satellite signals since we wanted to analyze the expected performance using authentication with Galileo OSNMA when it is fully operational (for details about these investigations, see [5]). The GNSS/IMU system was configured to record raw data (RINEX) of all GNSS systems with 1 Hz as well as IMU raw data with 500 Hz.

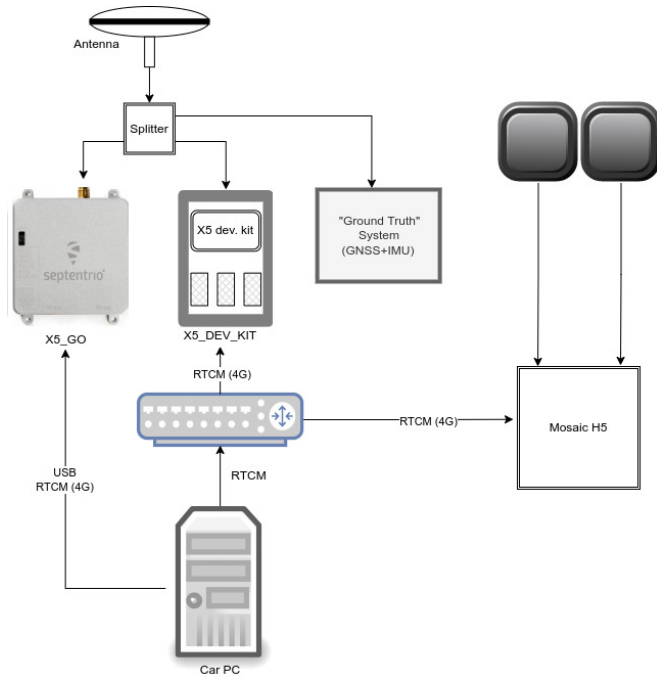


Figure 3. Automated Driving Demonstrator EGNSS architecture and interfaces.

### III. USE CASE

To analyze the effect of OSNMA authentication on positioning accuracy, a path-tracking use case was performed with and without OSNMA authentications. Path tracking is a classical topic in the control and robotics community where the exact localization of the robot with respect to a reference path is crucial to accomplish the path-following task. In the ESRIUM project, this topic is analysed in the context of automated driving systems since often the control task is rendered to that of following a reference path, which can either be obtained from onboard sensors or provided externally. Perhaps the best example of such an ADAS system in this context is the lane-keeping assistant (LKA) system, where the onboard sensors detect the adjacent lane markings to generate a reference path to follow for the AV [6].

The specific use case we implement in this context is illustrated in Figure 4, where the reference path is provided to the vehicle beforehand. The exact procedure to obtain the reference path is presented in Section III-B.

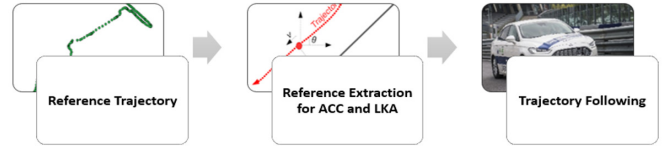


Figure 4. Path following use case implemented within the ESRIUM Project.

This implementation was then used in two different test cases, namely in an open-sky and urban location, with two different OSNMA settings to analyse its effect on the automated driving performance.

#### A. Driving function

To implement fully automated GNSS-based tracking of a given reference path, the driving function is composed of the following components:

- 1) A path follower function which finds the section of the reference path related to the current position of the vehicle.
- 2) A speed control function, which calculates a desired acceleration based on the deviation from the set speed and speed constraints due to the curvature of the path section from 1.
- 3) A lateral controller, which calculates the path tracking error and from that, the desired steering wheel angle  $\delta_{\text{set}}$ .
- 4) A longitudinal controller actuating the brake/throttle commands to regulate the vehicle's speed.

Components 2-4 have been successfully applied to other use cases previously. The longitudinal controller (4) is a standard PI controller outlined in [3]. The concept of the lateral controller was introduced in [7] and the actual implementation was recapitulated in [8]. In summary, a state-feedback control law

$$\delta_{\text{set}} = - [v_y \quad \dot{\psi} \quad e_{\text{lat}} \quad e_{\psi} \quad \chi] \mathbf{k}_{\text{lat}} \quad (1)$$

is obtained based on the linear single-track model [9], with the states lateral velocity  $v_y$  and yaw rate  $\dot{\psi}$ , and a linearized path tracking error model expressed by the lateral error  $e_{\text{lat}}$  and heading error  $e_{\psi}$ . The dynamics of the steering actuator are approximated by a first-order transfer function introducing the state  $\chi$ . The remaining details about the components 1 and 2 are shortly summarized in the following.

To find the section of interest of a parametric reference path  $\Gamma(\tau)$ , we first find the orthogonal projection of the current vehicle position  $\mathbf{p}$  with respect to the path, i.e. the path parameter  $\tau^*$  so that the orientation vector  $\Gamma'(\tau^*)$  of the path and the vector  $\mathbf{p} - \Gamma(\tau^*)$  are orthogonal:

$$\langle \Gamma'(\tau^*), \mathbf{p} - \Gamma(\tau^*) \rangle = 0. \quad (2)$$

For a polynomial spline, this results in a root-finding problem. Then the section of interest is found by restricting  $\Gamma(\tau)$  to the

domain  $\tau^* - a \leq \tau \leq \tau^* + b$ , where  $a > 0$  and  $b > 0$  are tunable parameters. The sectioning procedure was done in the Frenet frame allowing for an easy interpretation of parameters  $a$  and  $b$  in terms of a look-ahead and look-back distance along the path.

The speed control function first calculates an upper velocity threshold

$$v_{\max} = \sqrt{\frac{a_{y,\max}}{\kappa_{\max}}} \quad (3)$$

based on the maximum curvature  $\kappa_{\max} = \max(|\kappa(\tau)|)$  of the current path section with path parameter  $\tau$ . A tunable maximum lateral acceleration  $a_{y,\max} > 0$  ensures a comfortable ride at curvy sections. Then the desired acceleration is obtained from

$$a_{\text{set}} = k_p (\min\{v_{\text{set}}, v_{\max}\} - v), \quad (4)$$

where a proportional gain  $k_p$  weights the deviation of the actual velocity  $v$  from the desired velocity  $v_{\text{set}}$  saturated with the maximum velocity  $v_{\max}$ .

### B. Reference path

The reference path was obtained in the following way:

- 1) A manually driven trajectory was logged with a high-precision GNSS system.
- 2) The section of interest was extracted from the logged data resulting in a list of waypoints.
- 3) The final reference path was then obtained from a spline approximation algorithm [10].

The boundary conditions for the spline approximation were set so that the resulting reference path is a closed path which allowed to do several consecutive rounds of uninterrupted autonomous driving. This is important to obtain “steady state” path tracking results, as there was no measure implemented which guarantees the same initial conditions of the individual test runs.

The representation of the reference path as a polynomial spline was preferred over the list of waypoints because of its smoothness properties. A list of waypoints, assuming linear interpolation between consecutive waypoints, is only of zeroth parametric continuity ( $C^0$  continuous). However, the utilization of the path’s heading or curvature in the control law is a common technique [7], [11], [12] and discontinuities in the derivatives of the reference path might result in degraded path tracking performance [13]. In contrast, the polynomial spline allows for an arbitrary order of continuity. Specifically, a degree of 3 with  $C^2$  continuity at the knots was chosen for the polynomials, which implies differentiable heading and continuous curvature [14].

## IV. RESULTS

In this section, we present the results of the path following experiments with/without OSNMA localization. We also made the tests in two different settings, namely in open-sky and urban environments as shown in Figure 5, to analyze the effect of multi-path on the path following performance. These are described next.

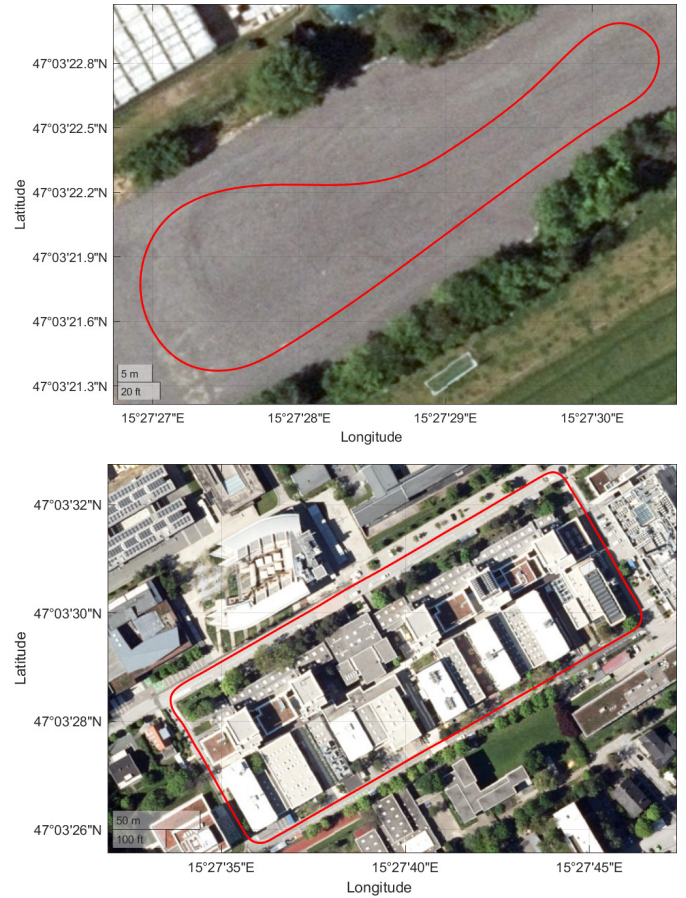


Figure 5. Bird’s eye view of the open-sky (top) and urban (bottom) environments with the added reference path (red).

### A. Open-sky Experiment

Figure 6 shows the path following results under open-sky with OSNMA disabled (blue) and OSNMA enabled (red). The first sub-figure on the top shows the reference path and the logged vehicle position. The sub-figures below show the steering wheel angle, look-ahead distance, lateral error  $e_{\text{lat}}$  and vehicle speed  $v$  in order from top to bottom. Four rounds of the circuit have been performed each for OSNMA-disabled and OSNMA-enabled settings.

The lateral error  $e_{\text{lat}}$  in Figure 6 shows several outliers at about 40 sec, 85 sec and 130 sec related to the tight U-turn in the upper right of the xy-plot. Analysis of the recorded data revealed, that these outliers were cause by a combination of an improperly tuned look-ahead distance, the path tracking error model used by the steering controller, as well as saturation of the control signal. The error model defines the reference point on the reference path as the intersection of the path with a line perpendicular to the vehicle heading at the look-ahead distance (see [7] for an illustration). The look-ahead distance of 3 m caused the vehicle to cut corners. But, due to saturation of the steering wheel angle, at the end of the U-turn the vehicle is almost perpendicular to the tangent of the respective path section, resulting in the outliers showing

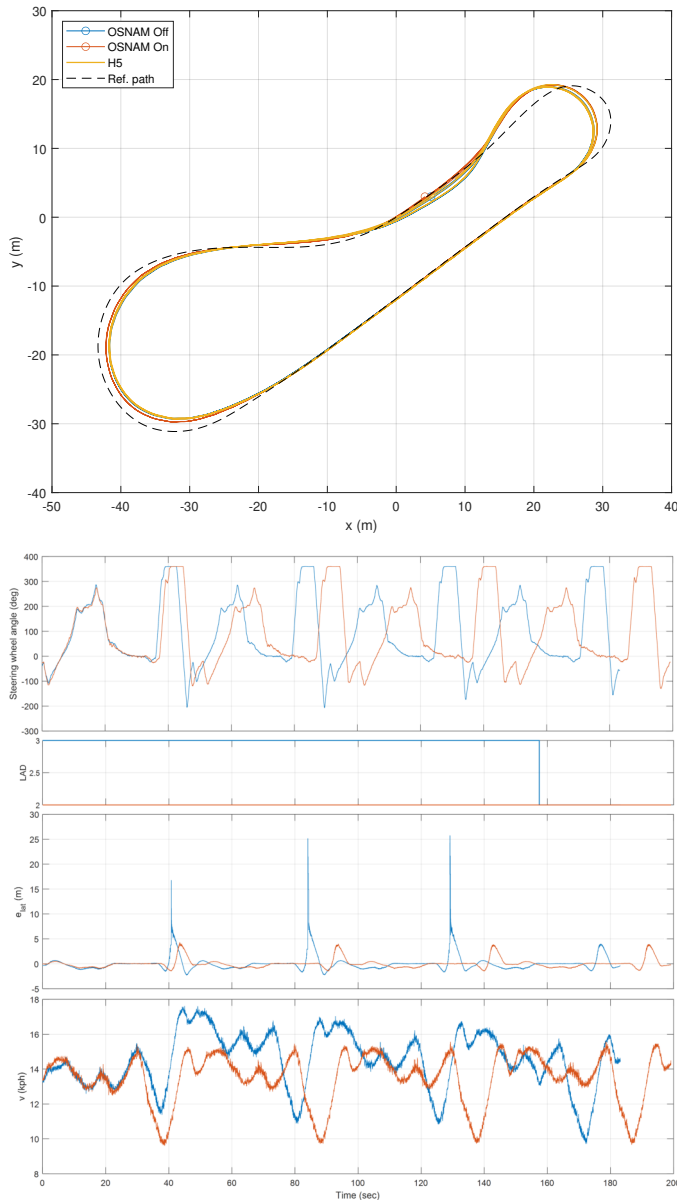


Figure 6. Comparison of OSNMA off (blue) and on (red) in the open-sky setting. The tracks with OSNMA on and off as opposed to the reference path are shown at the top. The steering wheel angle, look-ahead distance (LAD), lateral error and velocity are shown in order from top to bottom.

a lateral error of more than 15 m (with respect to the look-ahead point). On the other hand, the control signal was not saturated during the U-turn in the lower left corner. Therefore the vehicle did not cross the reference path and the lateral error was kept within a reasonable range of  $-1$  m to  $1$  m. The Figure also clearly shows, that a reduced look-ahead distance of 2 m as used throughout the OSNMA-on test and the end of the OSNMA-off test eliminated this problem, which can be explained by the definition of the path tracking error as mentioned above.

Besides these issues related to the path tracking implementation, especially the straight sections of the reference

path indicate, that the OSNMA feature does not influence the positioning accuracy. In general, considering that the OSNMA-on test compared to the OSNMA-off test is stretched along the time axis due to slight deviations of the vehicle speed, the trend of the lateral offset is quite similar between the two tests. Consequently, the same statement holds for the steering wheel angle as well as the velocity.

### B. Urban Driving Experiment

For the urban driving test case, a large loop within the Graz University of Technology Inffeldgasse campus as seen in Figure 7 was used. There are dense buildings and trees along this track to cause sufficiently high interference and multi-path reflections to degrade the GNSS location solution. During these experiments, OSNMA-on (which is only using enabled Galileo Satellites) setting provided no RTK-assisted solution. Therefore stable tracking was not possible due to positioning errors resulting from multi-path signals and the lack of sufficient visible satellites supporting OSNMA. In this case, path following only without OSNMA was tested. Even with OSNMA turned off, multi-path signals can cause deviations in sub-meter ranges, which affects GNSS-based tracking performance.

The general observation was that path following works but is not reliable due to the changing RTK localization types due to multi-path signals, indicating changeable or unstable positioning accuracy, thus resulting in wavy and unreliable tracking behaviour.

## V. CONCLUSIONS

In this paper, we have implemented a path-tracking controller for an automated driving demonstrator vehicle to test the effect of OSNMA authentication service in the context of automated vehicle localization. The experiments indicated that the use of OSNMA under open-sky conditions is feasible with limitations. Even with OSNMA turned off, sub-meter deviations can lead to control performance issues of the automated vehicle. This can be attributed to the very low number of OSNMA-enabled EGNSS satellites as well as the instantaneous changeability of the RTK solution method.

Particularly for urban settings, multi-path effects can lead to severe degradation in localization solutions, which exacerbates accuracy and tracking performance. In our experiments, the OSNMA strict setting was unusable in urban settings for accurate or improved localization and OSNMA-off was marginally usable but definitely not acceptable for stable path tracking purposes.

Since it is not possible with active OSNMA authentication to spoof position information, it brings some security assurance factors to satellite-based localization. However, the stable operation requires sufficient coverage and a clear line of sight with the sky. These factors severely limit the utility of GNSS-based localization systems for safety-related applications in automated driving solutions. For autonomous driving, OSNMA helps only marginally with the problem, though further

## REFERENCES

- [1] SAE-J3016, *Taxonomy and Definitions for Terms Related to Driving Automation Systems for On-Road Motor Vehicles*, Society of Automotive Engineers Standard, apr 2021.
- [2] ESRIUM-Project. (2020) EGNSS-enabled Smart Road Infrastructure usage and Maintenance for increased energy efficiency and safety on european road networks. Accessed: 2023-05-20. [Online]. Available: <https://esrium.eu/>
- [3] M. Rudigier, G. Nestlinger, K. Tong, and S. Solmaz, "Development and verification of infrastructure-assisted automated driving functions," *Electronics*, vol. 10, no. 17, 2021.
- [4] M. Rudigier, S. Solmaz, G. Nestlinger, and K. Tong, "Development, verification and KPI analysis of infrastructure-assisted trajectory planners," in *2022 International Conference on Connected Vehicle and Expo (ICCVE)*. IEEE, March 2022, pp. 1–6.
- [5] R. Lesjak, S. Schweitzer, J. M. V. García, K. Diengsleder-Lambauer, and S. Solmaz, "A comparative experimental performance assessment of RTK+OSNMA based positioning for road vehicle applications," in *Proceedings of the European Navigation Conference, ENC 2023*, Noordwijk, Netherlands, 2023.
- [6] S. Solmaz, G. Nestlinger, and G. Stettinger, "Compensation of sensor and actuator imperfections for lane-keeping control using a kalman filter predictor," *SAE International Journal of Connected and Automated Vehicles*, vol. 4, no. 1, pp. 97–106, mar 2021. [Online]. Available: <https://doi.org/10.4271/12-04-01-0008>
- [7] G. Nestlinger and M. Stolz, "Bumpless transfer for convenient lateral car control handover," *IFAC-PapersOnLine*, vol. 49, no. 15, pp. 132–138, 2016, 9th IFAC Symposium on Intelligent Autonomous Vehicles IAV 2016—Leipzig, Germany, 29 June–1 July 2016.
- [8] G. Nestlinger, J. Rumetshofer, and S. Solmaz, "Leader-based trajectory following in unstructured environments—from concept to real-world implementation," *Electronics*, vol. 11, no. 12, p. 1866, 2022.
- [9] P. Riekert and T. Schunck, "Zur fahrmechanik des gummibereiften kraftfahrzeugs," *Ingenieur-Archiv*, vol. 11, pp. 210–224, 1940.
- [10] N. Ezhov, F. Neitzel, and S. Petrovic, "Spline approximation, part 1: Basic methodology," *Journal of Applied Geodesy*, vol. 12, no. 2, pp. 139–155, apr 2018.
- [11] G. M. Hoffmann, C. J. Tomlin, M. Montemerlo, and S. Thrun, "Autonomous automobile trajectory tracking for off-road driving: Controller design, experimental validation and racing," in *2007 American Control Conference*. IEEE, jul 2007, pp. 2296–2301.
- [12] M. A. Zakaria, H. Zamzuri, R. Mamat, and S. A. Mazlan, "A path tracking algorithm using future prediction control with spike detection for an autonomous vehicle robot," *International Journal of Advanced Robotic Systems*, vol. 10, no. 8, p. 309, 2013.
- [13] J. Rumetshofer, M. Stolz, and D. Watenig, "A generic interface enabling combinations of state-of-the-art path planning and tracking algorithms," *Electronics*, vol. 10, no. 7, p. 26, mar 2021.
- [14] R. H. Bartels, J. C. Beatty, and B. A. Barsky, *An Introduction to Splines for Use in Computer Graphics & Geometric Modeling*. San Francisco, CA, USA: Morgan Kaufmann Publishers Inc., 1987.
- [15] "EPOSA web page," <https://www.eposa.at/>, accessed: 2023-05-15.

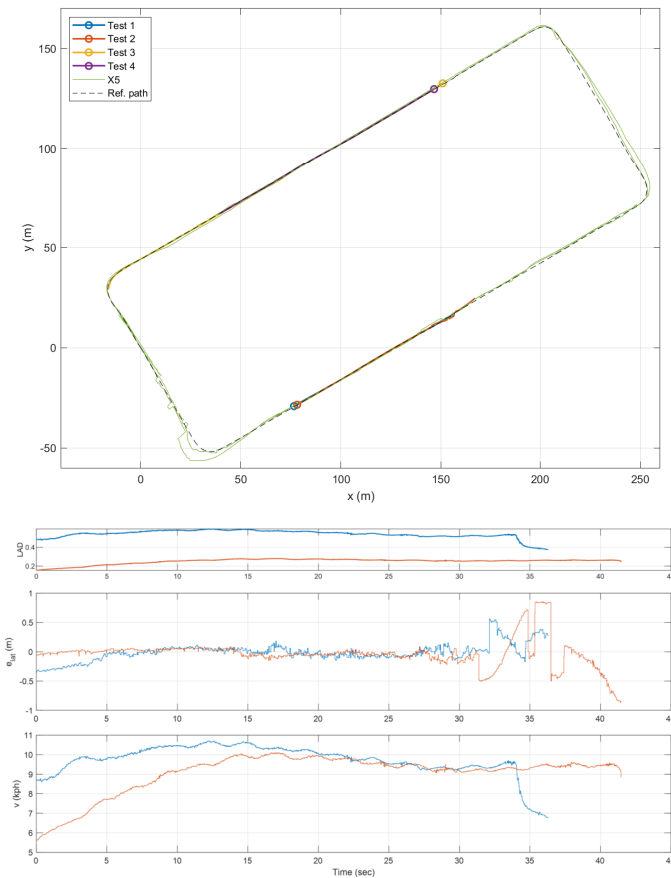


Figure 7. Urban driving experiment only with the OSNMA-off setting. Different colours indicate different runs on the same path.

testing needs to be done in more representative motorway conditions and with the presence of more supporting satellites.

## ACKNOWLEDGMENT

This work was conducted in the scope of the ESRIUM Project, which has received funding from the European Union Agency for the Space Programme under the European Union’s Horizon 2020 research and innovation programme and under grant agreement No 101004181. The content of this paper reflects only the authors’ view. Neither the European Commission nor the EUSPA is responsible for any use that may be made of the information it contains. Virtual Vehicle Research GmbH has received funding within COMET Competence Centers for Excellent Technologies from the Austrian Federal Ministry for Climate Action, the Austrian Federal Ministry for Labour and Economy, the Province of Styria (Dept. 12) and the Styrian Business Promotion Agency (SFG). The Austrian Research Promotion Agency (FFG) has been authorised for the programme management.

This project was supported by the Austrian RTK service provider EPOSA [15] providing their service free of charge.